Chapter 7
Many-Body Problems

So far, we have discussed only one-particle problems. We now turn our attention to cases in which more than one particle is present.

In the first place, we stress the fact that if $\hat{H} = \hat{H}(1) + \hat{H}(2)$, where $\hat{H}(1)$ and $\hat{H}(2)$ refer to different degrees of freedom (in particular, to different particles), and if $\hat{H}(1)\varphi_a(1) = E_a\varphi_a(1)$ and $\hat{H}(2)\varphi_b(2) = E_b\varphi_b(2)$, then

$$\begin{aligned} \varphi_{ab}(1,2) &= \varphi_a(1)\,\varphi_b(2), \\ \hat{H}\,\varphi_{ab}(1,2) &= (E_a + E_b)\,\varphi_{ab}(1,2). \end{aligned} \tag{7.1}$$

In the second place, we note that the distinction between identical particles is prevented in quantum physics by Heisenberg indeterminacy (unless they are wide apart). The quantum treatment of identical particles requires a new principle – the Pauli Principle – which is presented in Sect. 7.1. Particles can be either fermions or bosons.

In this chapter, we deal with many-body problems that are amenable to an independent-particle description. Central potentials in atomic and nuclear physics, electron gas and periodic potentials in solid state physics are fermion problems to be treated with methods developed in Chap. 6 and Sects. 4.4 and 4.6†. Problems involving phonons in lattices and condensation of bosons are dealt with by means of generalizations of the harmonic oscillator solution (Sect. 3.3.1). An exception is represented by the fractional Hall effect. Rather than presenting an overview of these many-body fields, we restrict ourselves to illustrate the quantum formalism with relevant applications. However, even this restricted framework allows us to introduce some of the most spectacular discoveries of the recent decades, which are based on quantum mechanics and are (or may become) cornerstones of present and future technologies: transistors, quantum dots, Bose–Einstein condensation and quantum Hall effects.

The concept of creation and annihilation operators is extended to many-body boson and fermion systems in Sect. 7.8†.

D. Bes, *Quantum Mechanics*, Graduate Texts in Physics,
DOI 10.1007/978-3-642-20556-9_7,

7.1 The Pauli Principle

Let us now consider the case of two identical particles, 1 and 2. Two particles are identical if their interchange, in any physical operator, leaves the operator invariant:

$$[\hat{P}_{12}, \hat{Q}(1,2)] = 0, \tag{7.2}$$

where $\hat{P}_{12}$ is the operator corresponding to the interchange process $1 \leftrightarrow 2$. As a consequence, the eigenstates of $\hat{Q}$ may be simultaneous eigenstates of $\hat{P}_{12}$ (Sect. 2.6.1). The operator $\hat{P}_{12}^2$ must have the single eigenvalue 1, since the system is left invariant by interchanging the particles twice. Thus the two eigenvalues of the operator $\hat{P}_{12}$ are ± 1. The eigenstates are said to be symmetric $(+1)$ or antisymmetric (-1) under the interchange of particles $1 \leftrightarrow 2$.

Consider two orthogonal single-particle states φ_p, φ_q which may be, in particular, eigenstates of a Hamiltonian. We construct the four two-body states by distributing the two particles in the two single-particle states. The symmetric combinations are

$$\Psi_{pp}^{(+)} = \varphi_p(1)\varphi_p(2), \tag{7.3}$$

$$\Psi_{qq}^{(+)} = \varphi_q(1)\varphi_q(2), \tag{7.4}$$

$$\Psi_{pq}^{(+)} = \frac{1}{\sqrt{2}}\Big[\varphi_p(1)\varphi_q(2) + \varphi_q(1)\varphi_p(2)\Big], \tag{7.5}$$

while the antisymmetric state is

$$\Psi_{pq}^{(-)} = \frac{1}{\sqrt{2}}\Big[\varphi_p(1)\varphi_q(2) - \varphi_q(1)\varphi_p(2)\Big]. \tag{7.6}$$

The states (7.5) and (7.6) are called entangled states, meaning that they are not simply written as a component of the tensor product of the state vectors of particle 1 and particle 2 (see Chap. 12).

The average distance between two entangled identical particles is

$$\langle pq|(\boldsymbol{r}_1 - \boldsymbol{r}_2)^2|pq\rangle_{(\pm)}^{1/2} = \Big(\langle p|r^2|p\rangle + \langle q|r^2|q\rangle - 2\langle p|\boldsymbol{r}|p\rangle\langle q|\boldsymbol{r}|q\rangle \mp 2\,|\langle p|\boldsymbol{r}|q\rangle|^2\Big)^{1/2}, \tag{7.7}$$

where the subscripts $(\pm)$ denote symmetric and antisymmetric states. The first three terms correspond to the average "classical" distance which is obtained if state functions of the type $\varphi_p(1)\varphi_q(2)$ are used. According to (7.7), this classical distance may be decreased for entangled particles in symmetric states and increased if they are in antisymmetric states. Therefore, the symmetry induces correlations between identical particles, even in the absence of residual interacting forces.

We now generalize the construction of symmetric and antisymmetric states to ν identical particles. Let $\hat{P}_b$ denote the operator that performs one of the $\nu!$ possible

permutations. It can be shown that this operator may be written as a product of two-body permutations $\hat{P}_{ij}$. Although this decomposition is not unique, the parity of the number η_b of such permutations is. We construct the operators

$$\hat{\mathcal{S}} \equiv \frac{1}{\sqrt{\nu!}} \sum_b \hat{P}_b, \qquad \hat{\mathcal{A}} \equiv \frac{1}{\sqrt{\nu!}} \sum_b (-1)^{\eta_b} \hat{P}_b. \tag{7.8}$$

Acting with the operator $\hat{\mathcal{S}}$ on a state of ν identical particles produces a symmetric state, while acting with $\hat{\mathcal{A}}$ produces an antisymmetric state.

A new quantum principle has to be added to those listed in Chap. 2:

Principle 4. *There are only two kinds of particles in nature*[1]*: bosons described by symmetric state vectors and fermions described by antisymmetric state vectors.*

As long as the Hamiltonian is totally symmetric in the particle variables, its eigenstates may be labeled with their properties under the interchange of two particles (symmetry or antisymmetry). According to Principle 4, many otherwise possible states are eliminated. For instance, the only two-body fermion state that can be found in nature is (7.6).

All known particles with half-integer values of spin are fermions (electrons, muons, protons, neutrons, neutrinos, etc.). All known particles with integer spin are bosons[2] (photons, mesons, etc.).

Moreover, every composite object has a total angular momentum, which can be viewed as the composite particle spin, and which is obtained according to the addition rules of Sect. 5.3.1. If this spin has a half-integer value, the object behaves like a fermion, whereas a composite system with an integer value of the spin acts as a boson. For instance, He^3 is a fermion (two protons and one neutron), while He^4 is a boson (an α-particle, with two protons and two neutrons), in spite of the fact that both isotopes have the same chemical properties.

Let us distribute ν identical bosons into a set of single-particle states φ_p and denote by n_p the number of times that the single-particle state p is repeated. The n_p are called occupation numbers. To construct the symmetrized ν-body state vector, we start from the product

$$\begin{aligned}\Psi_{pq\cdots r}(1,2,\ldots,\nu) &= \varphi_p(1)\varphi_p(2)\cdots\varphi_p(n_p)\varphi_q(n_p+1)\varphi_q(n_p+2)\cdots\varphi_q(n_p+n_q)\cdots\varphi_r(\nu) \\ &= \varphi_p^{(n_p)}\varphi_q^{(n_q)}\cdots\varphi_r^{(n_r)},\end{aligned} \tag{7.9}$$

[1] For the last 20 years it has been understood that, although this postulate holds true in our three-dimensional world, there is a whole range of intermediate possibilities – anyons – between bosons and fermions, in two dimensions. In some cases there are surface layers a few atoms thick in which the concept of anyons is realized, as in the fractional quantum Hall effect (Sect. 7.6.2†).

[2] Pauli produced a demonstration of this relation between spin and statistics which involved many complications of quantum field theory. Feynman's challenge that an elementary proof of the spin-statistics theorem be provided has not yet been answered.

with $\sum_i n_i = \nu$. Subsequently, the state vector is symmetrized by applying the operator $\hat{\mathcal{S}}$. The final state is

$$\Psi_{n_p,n_q,\ldots,n_r}(1,2,\ldots,\nu) = \mathcal{N}\hat{\mathcal{S}}\Psi_{pq\cdots r}(1,2,\ldots,\nu), \tag{7.10}$$

where $\mathcal{N}$ is a normalization constant. The occupation numbers label the states. There are no restrictions on the number of bosons in a given single-boson state. For instance, in the two-particle case, the possible symmetric state vectors are (7.3), (7.4) and (7.5).

We may also characterize the state by using the occupation numbers in the case of fermions. The procedure for constructing the antisymmetric state is the same, but for the application of the operator $\hat{\mathcal{A}}$ instead of $\hat{\mathcal{S}}$. However, the results are different, in the sense that occupation numbers must be 0 or 1. Otherwise the state vector would not change its sign under the exchange of two particles occupying the same state. The antisymmetrization principle requires that fermions should obey Pauli's exclusion principle [42]: "If there is an electron in the atom for which these [four] quantum numbers have definite values, then the state is occupied, full, and no more electrons are allowed in."

The antisymmetric state function for ν fermions may be written as a Slater determinant:

$$\Psi_{pq\cdots r}(1,2,\ldots,\nu) = \frac{1}{\sqrt{\nu!}}\begin{vmatrix} \varphi_p(1) & \varphi_p(2) & \cdots & \varphi_p(\nu) \\ \varphi_q(1) & \varphi_q(2) & \cdots & \varphi_q(\nu) \\ \vdots & \vdots & \ddots & \vdots \\ \varphi_r(1) & \varphi_r(2) & \cdots & \varphi_r(\nu) \end{vmatrix}. \tag{7.11}$$

The permutation of two particles is performed by interchanging two columns, which produces a change of sign. All the single-particle states must be different. Otherwise, the two rows are equal and the determinant vanishes.

A widely used representation of the states (7.9) and (7.11), in terms of creation and annihilation operators, is given in Sect. 7.8†.

The possibility of placing many bosons in a single (symmetric) state gives rise to phase transitions, with important theoretical and conceptual implications that are illustrated for the case of the Bose–Einstein condensation (Sect. 7.5†). Even more spectacular consequences appear in the fermion case.[3] Some of them will be treated later in this chapter.

[3]To reconcile the successes of the (fermion) quark model with the requirement that the total wave function be antisymmetric, it is necessary to hypothesize that each quark comes into three different species, which are labeled by the colors red, green and blue. Baryon wave functions may thus be antisymmetrized in color subspace.

7.2 Two-Electron Problems

Let us consider the case of the He atom. For the moment, we disregard the interaction between the two electrons. The lowest available single-particle states for the two electrons are the $\varphi_{100\frac{1}{2}m_s}$, $\varphi_{200\frac{1}{2}m_s}$ and $\varphi_{21m_l\frac{1}{2}m_s}$ states, where we use the same representation as in (6.10).

This problem involves four angular momenta: the two orbital and the two spin angular momenta. The two orbital angular momenta and the two spins may be coupled first[4] ($\hat{\boldsymbol{L}} = \hat{\boldsymbol{L}}_1 + \hat{\boldsymbol{L}}_2$ and $\hat{\boldsymbol{S}} = \hat{\boldsymbol{S}}_1 + \hat{\boldsymbol{S}}_2$). Subsequently, the addition of the total orbital and total spin angular momenta yields the total angular momentum $\hat{\boldsymbol{J}} = \hat{\boldsymbol{L}} + \hat{\boldsymbol{S}}$.

The spin part of the state vector may carry spin 1 or 0. We obtain the corresponding states $\chi^s_{m_s}$ by using the coupling given in (5.67), with $j_1 = j_2 = 1/2$. The (three) two-spin states with spin 1 are symmetric, while the state with spin 0 is antisymmetric. Thus,

$$\chi^1_1(1,2) = \varphi_\uparrow(1)\varphi_\uparrow(2), \qquad \chi^1_0(1,2) = \frac{1}{\sqrt{2}}\Big[\varphi_\uparrow(1)\varphi_\downarrow(2) + \varphi_\uparrow(2)\varphi_\downarrow(1)\Big],$$
$$\chi^1_{-1}(1,2) = \varphi_\downarrow(1)\varphi_\downarrow(2), \qquad \chi^0_0(1,2) = \frac{1}{\sqrt{2}}\Big[\varphi_\uparrow(1)\varphi_\downarrow(2) - \varphi_\uparrow(2)\varphi_\downarrow(1)\Big]. \tag{7.12}$$

We now consider different occupation numbers for the two electrons:

1. The two electrons occupy the lowest orbit $\varphi_{100\frac{1}{2}m_s}$. In this case, the spatial part is the same for both electrons and, thus, the state vector is necessarily spatially symmetric. Therefore the symmetric spin state with spin 1 is excluded by the exclusion principle. Only the (entangled) state with zero spin can exist.
2. One electron occupies the lowest level $\varphi_{100\frac{1}{2}m_s}$ and the other, the next level $\varphi_{200\frac{1}{2}m_s}$. In this case, the difference in the radial wave functions allows us to construct both a symmetric and an antisymmetric state for the spatial part of the wave function [(7.5) and (7.6), respectively]. Both spatial states carry $l = 0$. Two total states are now allowed by the Pauli principle: the combination of the symmetric spatial part with the antisymmetric spin state and vice versa. The (so far neglected) interaction between the electrons breaks the degeneracy between these two allowed total states: according to (7.7), two electrons in a spatially antisymmetric state are further apart than in a symmetric state. They thus feel less

[4] There is an alternative coupling scheme in which the orbital and spin angular momenta are first coupled to yield the angular momentum of each particle: $\hat{\boldsymbol{J}}_i = \hat{\boldsymbol{L}}_i + \hat{\boldsymbol{S}}_i$ ($i = 1, 2$), as in (6.11). Subsequently, the two angular momenta are coupled together: $\hat{\boldsymbol{J}} = \hat{\boldsymbol{J}}_1 + \hat{\boldsymbol{J}}_2$. The two coupling schemes give rise to two different sets of basis states.

Coulomb repulsion. Their energy decreases relative to the energy of the spatially symmetric state.

3. One electron occupies the lowest level $\varphi_{100\frac{1}{2}m_s}$ and the other, the level $\varphi_{21m_l\frac{1}{2}m_s}$. It is left for the reader to treat this case as an exercise. He or she may follow the same procedure as in the previous example, bearing in mind that the orbital angular momentum no longer vanishes.

7.3 Periodic Tables

7.3.1 The Atomic Case

The attraction exerted by the nuclear center, proportional to Ze^2, allows us to implement a central-field description for atomic systems displaying more than one electron. However, the Hamiltonian also includes the Coulomb repulsion between electrons. This interaction is weaker (since it is only proportional to e^2), but an electron experiences $Z-1$ such repulsions. We can nonetheless take them into account to a good approximation by modifying the central field because:

- Electrons from occupied levels cannot be scattered to other occupied levels (Pauli principle) and when scattered to empty levels have to overcome the gap between the energy of the occupied level and the energy of the last filled state, thus reducing the effectiveness of the residual interaction.
- The electric fields created by electrons lying outside a radius r' tend to cancel for radius $r < r'$, due to the well-known compensation between the field intensity ($\propto 1/r^2$) and the solid angle ($\propto r^2$).

Although the optimum choice of the single-particle central potential constitutes a more difficult problem (see Sect. 8.6.1† on the Hartree–Fock approximation), it is simple to obtain the behavior at the limits

$$\lim_{r\to 0} V(r) = -\frac{Ze^2}{4\pi\epsilon_0 r}, \qquad \lim_{r\to\infty} V(r) = -\frac{e^2}{4\pi\epsilon_0 r}. \tag{7.13}$$

Close to the nucleus, the electron feels all the nuclear electric field. Far away, this field is screened by the remaining $Z-1$ electrons. The potential at intermediate points may be obtained qualitatively by interpolation.

The energy eigenvalues of this effective potential are also qualitatively reproduced by adding the term

$$\hat{H}_l = c\hat{L}^2 \tag{7.14}$$

to the Coulomb potential, since the centrifugal term $\hbar^2 l(l+1)/2Mr^2$ prevents the electrons occupying levels with large values of l from approaching the center and, thus, feeling the greater attraction of the potential at small radii.

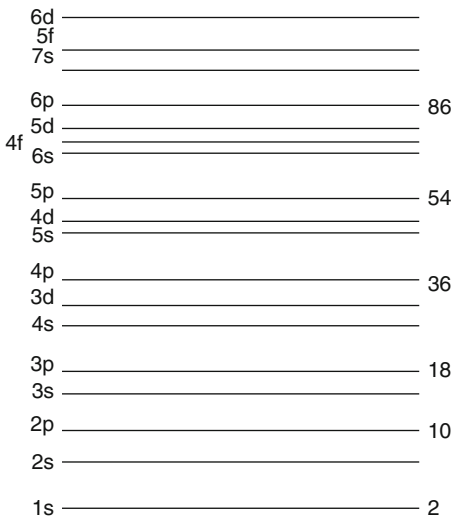

Fig. 7.1 Electron shell structure. The figure gives a rough representation of the order of single-electron levels. Numbers to the *right* indicate the number of electrons in closed shell atoms

The energies E_{nl} are also labeled by the orbital quantum number, since the potential is no longer simply proportional to $1/r$ (Sect. 6.1.1). They are qualitatively presented in Fig. 7.1, where the nomenclature of Table 5.2 is used. The set of energy levels which are close to each other is called a shell. In a closed shell, all magnetic substates are occupied.

The ground state of a given atom is determined by successively filling the different single-particle states until the Z electrons are exhausted. A closed shell carries zero orbital and zero spin angular momenta (see Problem 7). A closed shell displays neither loose electrons nor holes, and thus constitutes a quite stable system. This fact explains the properties of noble gases in the Mendeleev chart, for which $Z = 2$, 10, 18, 36, 54 and 86 (Fig. 7.1). The angular momenta (including the magnetic momenta), the degree of stability, the nature of chemical bonds and, in fact, all the chemical properties are determined by the outer electrons lying in the last, unfilled shell, a spectacular consequence of the Pauli principle.

The electron configuration of an atom with many electrons is specified by the occupation of the single-particle states of the unfilled shell. For instance, the lowest configuration in the Mg atom, with $Z = 12$, is[5] $(3s)^2$. Configurations $(3s)(3p)$ and $(3p)^2$ lie close in energy.

In the atomic case the total single-particle angular momentum j is not usually specified (as it was not in Sect. 7.2), because the strength of the spin–orbit coupling is small relative to the electron repulsions. However, for heavier elements and inner shells, the quantum numbers (l, j) become relevant once again.

[5]The first number is the Coulomb principal quantum number; the orbital angular momentum follows the notation of Table 5.2; the exponent (2) denotes the number of particles with the previous two quantum numbers.

7.3.2 The Nuclear Case

Let us now consider the nuclear table. A nucleus has A nucleons, of which N are neutrons and Z are protons. Nuclei with the same A are called isobars; with the same N, isotones and with the same Z, isotopes. In spite of the fact that there is no *ab initio* attraction from a nuclear center and the internuclear force is as complicated as it can be, the Pauli principle is still effective: the starting point for the description of most nuclear properties is a shell model. For systems with short-range interactions, a realistic central potential follows the probability density, which in the nuclear case has a Woods–Saxon shape, $w(r)$ (Fig. 7.3). A strong spin–orbit interaction must be included on the surface, with an opposite sign to the atomic case. A central Coulomb potential also appears for protons

$$\hat{V} = -v_0 w(r) - v_{\rm so} \frac{r_0^2}{r} \frac{{\rm d}w(r)}{{\rm d}r} \hat{\boldsymbol{L}} \cdot \hat{\boldsymbol{S}} + V_{\rm coul}$$

$$w(r) \equiv \left(1 + \exp \frac{r - R}{a}\right)^{-1}. \tag{7.15}$$

The empirical values of the parameters appearing in (7.15) are [38]

$$v_0 = \left(-51 + 33 \frac{N - Z}{A}\right) \text{ MeV} \quad \text{and} \quad v_{\rm so} = 0.44 v_0.$$

Here $a = 0.67$ F represents the skin thickness and $R = r_0 A^{1/3}$ is the nuclear radius, with $r_0 = 1.20$ F. The resulting shell structure is shown in Fig. 7.2.

Nucleons moving in a Woods–Saxon potential see a potential similar to the harmonic oscillator potential (Fig. 7.3). An attractive term of the form (7.14) should also be included, since the nuclear single-particle states in which nucleons lie close to the surface are more energetically favored by the Woods–Saxon potential than by the harmonic oscillator potential (Fig. 7.3). Therefore, the simpler effective potential

$$\hat{V} = \frac{M_{\rm p} \omega^2}{2} r^2 - c \hat{\boldsymbol{L}} \cdot \hat{\boldsymbol{S}} - d \left(\hat{L}^2 - \langle L^2 \rangle_N\right) \tag{7.16}$$

may be used instead of (7.15), at least for bound nucleons, where $\hbar\omega = 41$ MeV $A^{-1/3}$, $c = 0.13\omega/\hbar$, and $d = 0.038\omega/\hbar$ for protons and $d = 0.024\omega/\hbar$ for neutrons ([38], Chap. 2). The symbol $\langle L^2 \rangle_N$ denotes the average value of L^2 in an N-oscillator shell (Problem 3 of Chap. 6). The eigenstates are labeled with the quantum numbers $Nljm\tau$, where the new quantum number τ equals $1/2$ for neutrons and $-1/2$ for protons.

The lowest shell $N = 0$ is filled up with four nucleons, two protons and two neutrons, giving rise to the very stable α-particle. As in the electron case, closed shells do not contribute to the properties of low-lying excited states. Note that both nucleons should fill closed shells to obtain the analogy of noble gases. This occurs

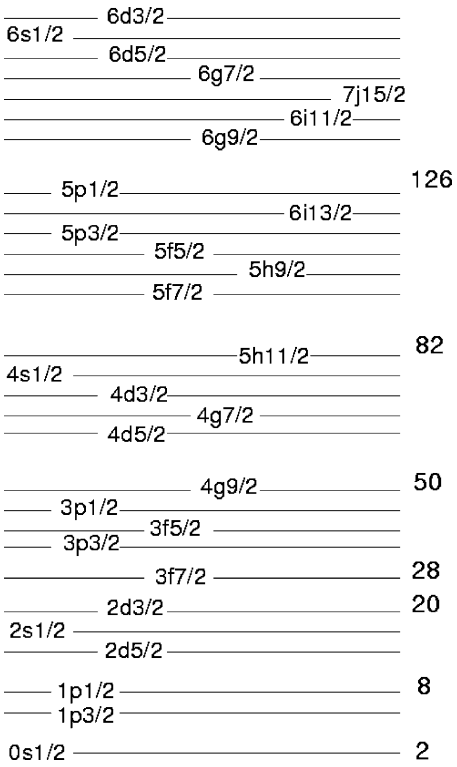

Fig. 7.2 Nuclear shell structure. This figure is an approximation of the order of single-nucleon levels. They are labeled with the quantum numbers Nlj. The number of nucleons for closed shell systems is indicated on the *right*

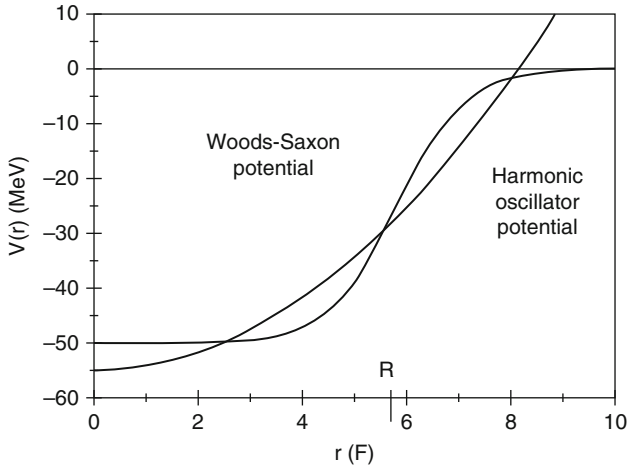

Fig. 7.3 Comparison of the Woods–Saxon and harmonic oscillator potentials [38]

Table 7.1 Levels of Sn^{133} populated by transferring a neutron from the deuteron target to the closed shell Sn^{132}. Energies in keV

Level	Energy	S
5f7/2	g.s.	0.86 ± 0.16
5p3/2	854	0.92 ± 0.18
5p1/2	1,363	1.1 ± 0.3
5f5/2	2,005	1.1 ± 0.2

in the nuclear systems $Z = N = 2$; $Z = N = 8$; $Z = N = 20$; $Z = 20, N = 28$; $Z = N = 28$; $Z = N = 50$; $Z = 50, N = 82$ and $Z = 82, N = 126$.

It should be stressed that, unlike the hydrogen case, the description of heavier atoms/nuclei in terms of a central field is, at best, a semi-quantitative approximation: one-body terms can never completely replace two-body interactions. The approximation is more reliable for systems that have one more particle (or hole) than a closed shell. In fact, the single-particle spectrum can be determined by transferring one nucleon to the double closed shells, as in (d,p) reactions. For instance, the spectroscopic factor (the ratio between experimental and predicted cross sections) should be $S = 1$ if the single-particle states are pure, without admixtures of core excitations.

Recently, single-particle levels above the double closed shell nucleus $Z = 50$, $N = 82$ (mean lifetime of 40 s) have been measured [43]. Since it is not possible to make a target with such a short-lived nucleus, a beam of Sn^{132} has been runned upon a deuterium target. The Sn^{133} levels are disentangled through properties of the scattered protons (intensities, energies, angular distributions). The results are given in Table 7.1 and agree, within expectations, with predictions from Fig. 7.2.

7.4 Motion of Electrons in Solids

7.4.1 Electron Gas

In the simplest possible model of a metal, electrons move independently of each other. The electrostatic attraction of the crystalline lattice prevents them from escaping when they approach the surface. The electron gas results of Sect. 4.4.1 may be easily generalized to the three-dimensional case. The wave states are given as the product of three one-dimensional solutions (4.43)

$$\varphi_{n_x n_y n_z} = \frac{1}{\sqrt{V}} \exp\left[\mathrm{i}(k_{n_x} x + k_{n_y} y + k_{n_z} z)\right]. \tag{7.17}$$

The volume is $V = a^3$. The allowed $\boldsymbol{k}$ values constitute a cubic lattice in which two consecutive points are separated by the distance $2\pi/a$ (4.42)

$$k_{n_i} = \frac{2\pi}{a} n_i, \qquad n_i = 0, \pm 1, \pm 2, \ldots, \quad i = x, y, z. \tag{7.18}$$

The energy of each level is

$$\epsilon_k = \frac{\hbar^2 |\boldsymbol{k}|^2}{2M}. \tag{7.19}$$

To build the ν-electron ground state, we start by putting two electrons on the level $k_x = k_y = k_z = 0$. We successively fill the unoccupied levels as their energy increases. When there is a large number of electrons, the occupied region will be indistinguishable from a sphere in k-space. The radius of this sphere is called k_F, the Fermi momentum, and its energy $\epsilon_\mathrm{F} \equiv \hbar^2 k_\mathrm{F}^2 / 2M$, the Fermi energy. At zero energy, the levels with $|\boldsymbol{k}| \leq k_\mathrm{F}$ are occupied pairwise and those above are empty. Since we are interested in the large-volume limit, the levels are very close together and we may replace summations with integrals that have a volume element similar to (4.45). Thus,

$$\sum_k f_k \approx \frac{V}{8\pi^3} \int f_k \, \mathrm{d}^3 k. \tag{7.20}$$

An electron gas is characterized by the Fermi temperature $T_\mathrm{F} \equiv \epsilon_\mathrm{F} / k_\mathrm{B}$, where k_B is the Boltzmann constant (Table A.1). If the temperature $T \ll T_\mathrm{F}$, the electron gas has properties that are very similar to the $T = 0$ gas. The number of levels per unit volume with energy less than ϵ and the density of states per unit interval of energy per unit volume are

$$n(\epsilon) = \frac{2}{V} \sum_{n_x n_y n_z} \approx \frac{1}{4\pi^3} \int_{k \leq k_\epsilon} \mathrm{d}^3 k = \frac{k_\epsilon^3}{3\pi^2} = \frac{1}{3\pi^2} \left(\frac{2M\epsilon}{\hbar^2} \right)^{3/2},$$

$$\rho(\epsilon) = \frac{\partial n}{\partial \epsilon} = \frac{1}{\pi^2 \hbar^3} \left(2M^3 \epsilon \right)^{1/2}, \tag{7.21}$$

respectively. At the Fermi energy, the values of these quantities are

$$n_\mathrm{F} = \frac{1}{3\pi^2} k_\mathrm{F}^3, \qquad \rho_\mathrm{F} = \frac{3 n_\mathrm{F}}{2\epsilon_\mathrm{F}}. \tag{7.22}$$

For the Na typical case: $n_\mathrm{F} \approx 2.65 \times 10^{22}$ electrons/cm^3, $k_\mathrm{F} \approx 0.92 \times 10^8$ cm^{-1}, $\epsilon_\mathrm{F} \approx 3.23$ eV and $T_\mathrm{F} \approx 3.75 \times 10^4$ K.

We now explore some thermal properties of an electron gas. If the electrons would obey classical mechanics, each of them should gain an energy of the order of $k_\mathrm{B} T$ in going from absolute zero to the temperature T. The total thermal energy per unit volume of electron gas would be of the order of

$$u_{\mathrm{cl}} = n_{\mathrm{F}} k_{\mathrm{B}} T, \tag{7.23}$$

and the specific heat at a constant temperature would thus be independent of the temperature:

$$(C_V)_{\mathrm{cl}} = \frac{\partial u_{\mathrm{cl}}}{\partial T} = n_{\mathrm{F}} k_{\mathrm{B}}. \tag{7.24}$$

However, the Pauli principle prevents most of the electrons from gaining energy. Only those with an initial energy ϵ_k such that $\epsilon_{\mathrm{F}} - \epsilon_k < k_{\mathrm{B}} T$ can be expected to gain energy. The number of such electrons is given roughly by

$$\rho_{\mathrm{F}} k_{\mathrm{B}} T = \frac{3 n_{\mathrm{F}}}{2} \frac{T}{T_{\mathrm{F}}}. \tag{7.25}$$

The total thermal energy and specific heat per unit volume are

$$u = \rho_{\mathrm{F}} (k_{\mathrm{B}} T)^2, \tag{7.26}$$

$$C_V = 3 n_{\mathrm{F}} k_{\mathrm{B}} \frac{T}{T_{\mathrm{F}}}. \tag{7.27}$$

The specific heat is proportional to the temperature and is reduced by a factor $\approx 1/100$ at room temperature.

The probability of an electron being in a state of energy ϵ is given by the Fermi–Dirac distribution $\eta(\epsilon)$ (7.55). Using this distribution, the expression for the total energy per unit volume is

$$u = \frac{1}{2\pi^2} \int_0^\infty \epsilon \, \rho(\epsilon) \, \eta(\epsilon) \, k^2 \, \mathrm{d}k, \tag{7.28}$$

which is a better approximation than (7.26). Upon integration, one obtains results similar to (7.27).

7.4.2† Band Structure of Crystals

Although the electron gas model explains many properties of solids, it fails to account for electrical conductivity, which can vary by a factor of 10^{30} between good insulators and good conductors.

A qualitative understanding of conductors and insulators may be obtained from a simple generalization of the band model described in Sect. 4.6†. As a consequence of the motion of single electrons in a periodic array of ions, the possible individual energies are grouped into allowed bands. Each band contains $2N$ levels, where N is the number of ions, and the factor 2 is due to spin.

According to the Pauli principle, we obtain the ground state by successively filling the individual single-particle states of the allowed bands. The last filled band is called the valence band. If we place the solid within an electric field, the electrons belonging to a valence band cannot be accelerated by a small electric field, since they would tend to occupy other states of the same band, which are already occupied. Much like the case of closed shells in atoms and nuclei, electrons in a valence band constitute an inert system which do not contribute to thermal or electrical properties. A solid consisting only of filled bands is an insulator. The insulation gets better as the distance ΔE between the upper valence band and the next (empty) band increases.

By contrast, electrons in partially filled bands can easily absorb energy from an applied electric field. Such a band is called a conduction band.

The previous considerations are valid for $T = 0$. In solids which are insulators at $T = 0$, the thermal motion increases the energy of the electrons by an amount $k_B T$. As the temperature increases, some electrons belonging to the valence band may jump to the conduction band. This system is a semiconductor. The conductivity varies as $\exp(-\Delta E / k_B T)$.

The existence of conductors, semiconductors and insulators is a consequence of the Pauli principle. Another consequence arises from the fact that the electrons which jump to the conduction band leave empty states called holes in the valence band. Other electrons of the same valence band may occupy these holes, leaving other holes behind them. Thus there is a current, due to the electrons of the valence band, which is produced by the holes. The holes carry a positive charge, because they represent the absence of an electron.

7.4.3† Transistors

Semiconductors have become key parts of electronic circuits and optical applications in modern electronic industry, due to the fact that their electrical conductivity can be greatly altered by means of external stimuli (voltage, photon flux, etc.) and by the introduction of selected impurities (doping).

There are different kinds of transistors, each one having different applications. Here we outline one of them, the metal-oxide semiconductor field effect transistor (MOSFET).

We denote by n a semiconductor with electrons at the conduction band and by p, one with holes at the valence band (Sect. 7.4.2†). As most transistors, the MOSFET consists of a sandwich made up by three semiconductors, the middle one being of different type than the other two (Fig. 7.4). On top there is an insulator followed by a metallic layer. If the control voltage applied between the metal and the bottom of the transistor vanishes, there is no electron output current flowing from left to right. However, if the bottom is at a negative potential, the positive free charges (holes) get attracted to it, and the output current flows on top, below the insulator layer. The output power can be much greater than at the control circuit.

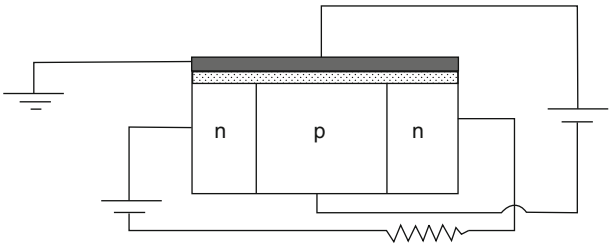

Fig. 7.4 Diagram of a MOSFET transistor

Weak voltage signals, arising from an antenna, can replace the control voltage and get amplified by a transistor. This is the role of transistors at your TV set. The MOSFET can also be used as a classical bit of your PC, the control voltage allowing (or not) the current to flow. They also play the role of switches.

Because of their flexibility, reliability and low cost, transistors are the building blocks of modern electronic circuits. They are used either as isolated units or as parts of integrated circuits (chips). Transistors were invented by John Bardeen, Walter Brattain and William Shockley at the Bell Labs in 1947.

7.4.4† Phonons in Lattice Structures

Up to now we have treated the ions as fixed in space at positions $\mathbf{R}_i$, giving rise to the crystal lattice structure. This is a consequence of the much larger ion mass M_I relative to the electron mass M. Subsequently we allow for a small fluctuation $\mathbf{u_i}$ in the coordinate $\mathbf{r}_i = \mathbf{R}_i + \mathbf{u}_i$ of the i ion (Born–Oppenheimer approximation). For the sake of simplicity, we make the following approximations:

- A linear, spinless chain of N ions separated by the distance d.
- Only terms up to quadratic order in u_i are kept in the ion–ion potential. Linear terms in the fluctuations vanish due to the equilibrium condition and the constant, equilibrium term will be dropped.
- Only interactions between nearest neighbors are considered.

Therefore, the Hamiltonian reads

$$\begin{aligned}\hat{H} &= \frac{1}{2M_I}\sum_i \hat{p}_i^2 + \frac{M_I\omega^2}{8}\sum_{i,j}\left(u_i - u_j\right)^2 \delta_{i(j\pm1)} \\ &= \frac{1}{2M_I}\sum_i \hat{p}_i^2 + \frac{M_I\omega^2}{2}\sum_i \hat{u}_i^2 - \frac{M_I\omega^2}{2}\sum_i u_i u_{i+1} \\ &= \hbar\omega\sum_i\left(a_i^+ a_i + \frac{1}{2}\right) - \frac{\hbar\omega}{4}\sum_i\left(a_i^+ + a_i\right)\left(a_{i+1}^+ + a_{i+1}\right), \qquad (7.29)\end{aligned}$$

where the creation and annihilation operators[6] a_i^+, a_i are defined as in (3.29) for each site i. The strength parameter ω in the ion–ion potential may be interpreted as the frequency of each oscillator in the absence of coupling with other oscillators.

As in classical physics, the coupled oscillators may become uncoupled by means of a linear transformation

$$\hat{H} = \hbar\omega_k \left(\gamma_k^+ \gamma_k + \frac{1}{2}\right)$$
$$\gamma_k^+ = \sum_i (\lambda_{ki} a_i^+ - \mu_{ki} a_i), \qquad \sum_i (\lambda_{ki}\lambda_{li}^* - \mu_{ki}\mu_{li}^*) = \delta_{kl}. \tag{7.30}$$

The uncoupling procedure is described at the end of the section. The resultant amplitudes λ_{ki}, μ_{ki} and the new frequencies ω_k are

$$\lambda_{ki} = \frac{1}{2}\left(\sqrt{\frac{\omega}{\omega_k N}} + \sqrt{\frac{\omega_k}{\omega N}}\right) \exp(ikr_i),$$
$$\mu_{ki} = \frac{1}{2}\left(\sqrt{\frac{\omega}{\omega_k N}} - \sqrt{\frac{\omega_k}{\omega N}}\right) \exp(ikr_i),$$
$$\omega_k = \frac{1}{\sqrt{2}}\,\omega\, k\, d, \tag{7.31}$$

where the frequencies ω_k are proportional to the wave number k. If a cyclic chain is assumed ($r_{N+1} = r_1$, see Sect. 4.4.1)

$$k = k_n = \frac{2\pi\, n_k}{N\, d}, \qquad n_k = 0. \pm 1, \pm 2, \ldots. \tag{7.32}$$

Thus, there are not only electrons and ions in a crystal but also extended periodic boson structures called phonons are present as well. According to (7.1), the phonon eigenstates and energies are given by[7]

$$\Psi = \prod_k \varphi_{n_k} = \prod_k \frac{1}{\sqrt{n_k!}} (\gamma_{n_k}^+)^{n_k} |0\rangle, \tag{7.33}$$

$$E(n_k) = \sum_k \hbar w_k \left(n_k + \frac{1}{2}\right). \tag{7.34}$$

These lattice vibrations have consequences on the thermodynamic properties of crystals, and in particular on the specific heat: because of the linear dependence of

[6] See also Sect. 7.8†.

[7] See also Sect. 7.8†.

frequency[8] on momentum, we can ignore the occupancy of other, finite frequency modes, if the thermal frequency $k_B T/\hbar$ is sufficiently small. To obtain the total phonon energy per unit volume V, we replace the phonon occupancies n_k in (7.34) by the thermal occupancy η_k given by the Bose–Einstein distribution (7.53)

$$\begin{aligned} u_{\text{phonon}} &= \frac{\hbar\alpha}{V}\sum_k k\left[\frac{1}{\exp\left(\frac{\hbar\alpha k}{k_B T}\right)-1}+\frac{1}{2}\right] \\ &\to \frac{\hbar\alpha}{2\pi^2}\int_0^\infty \frac{k^3 \mathrm{d}k}{\exp\left(\frac{\hbar\alpha k}{k_B T}\right)-1}+\frac{\hbar\alpha}{2V}\sum_k k \\ &= \frac{\pi^2 (k_B T)^4}{30(\hbar\alpha)^3}+\frac{\hbar\alpha}{2V}\sum_k k. \end{aligned} \tag{7.35}$$

Therefore, the phonon contribution to the specific heat at small T (well below room temperature) is proportional to T^3.

The Uncoupling of the Hamiltonian

The amplitudes λ_{ki}, μ_{ki} and the frequencies ω_k are determined by solving the harmonic oscillator equation

$$[\hat{H}, \gamma_k^+] = \hbar\omega_k \gamma_k^+. \tag{7.36}$$

Using the last line of (7.29) with this equation, one obtains

$$\begin{aligned} &(\hbar\omega - \hbar\omega_k)\sum_i \lambda_{ki} a_i^+ + (\hbar\omega + \hbar\omega_k)\sum_i \mu_{ki} a_i \\ &= \frac{\hbar\omega}{4}\sum_i (\lambda_{ki}+\mu_{ki})\left(a_{i-1}^+ + a_{i-1} + a_{i+1}^+ + a_{i+1}\right) \\ &= \frac{\hbar\omega}{4}\sum_i \left(\lambda_{k(i+1)}+\mu_{k(i+1)}+\lambda_{k(i-1)}+\mu_{k(i-1)}\right)\left(a_i^+ + a_i\right). \end{aligned} \tag{7.37}$$

Since a_i^+, a_i represent independent degrees of freedom, their coefficients in the first line of (7.37) should equal those in the third line. This requirement yields N sets of two homogeneous linear equations

[8] This linearity also holds in three dimensions (sound waves).

$$\lambda_{ki} - \mu_{ki} = \frac{w_k}{\omega}\,(\lambda_{ki} + \mu_{ki})\,,$$

$$\begin{aligned}\lambda_{ki} + \mu_{ki} &= -\frac{\omega^2}{2\omega_k^2}(\lambda_{k(i+1)} + \mu_{k(i+1)} + \lambda_{k(i-1)} + \mu_{k(i-1)} - 2\lambda_{ki} - 2\mu_{ki}) \\ &\approx -\frac{\omega^2 d^2}{2\omega_k^2}\,\frac{\mathrm{d}^2\,(\lambda_{ki} + \mu_{ki})}{(\mathrm{d}\,r_i)^2}\,. \end{aligned} \tag{7.38}$$

The last equation implies the frequencies given in the last line of (7.31) and

$$\lambda_{ki} + \mu_{ki} = \mathcal{N} \exp(\mathrm{i}k r_i)\,, \tag{7.39}$$

where $\mathcal{N}$ is a normalization constant. The normalization condition in (7.30) and the first of equations (7.38) yield the amplitudes (7.31).

This method of uncoupling constitutes a particular application of the random-phase approximation, a standard procedure in many-body physics (Sect. 8.6.2†).

7.4.5† Quantum Dots

Quantum dots, also called artificial atoms, are small regions (from 1 to about 100 nm; 1 nm = 10^{-9} m) of one semiconductor material buried in another semiconductor material with a larger energy gap ΔE (Sect. 7.4.2†). They are made up by roughly 10^6 atoms. In addition, quantum dots contain a controlled number of electrons that display atomic-like spectra with very sharp discrete lines (like natural atoms do). However, unlike natural atoms, their energies can be strongly influenced by the size of the dot and other interactions with the surroundings.

Electrons in a layer of GaAs are sandwiched between two layers of insulating AlGaAs, acting as tunnel barriers. One of these barriers is connected to the source lead, the other to the drain lead. The entire structure may also be linked to an insulated metal electrode which fixes the bias potential V_g.

The forces acting on the electrons inside the dot are difficult to estimate. However, it is possible to apply the concept of a central confining potential as in Sect. 7.3. When an electron enters or leaves the quantum dot there is a noticeable change in the capacitance of the dot, which can be measured. In Fig. 7.5 the capacitance is plotted against the voltage V_g. Each maxima denotes the loading of an additional electron to the dot. The first two electrons fill the lowest, spin degenerate states. The next shell displays four equally spaced maxima, which is consistent with a harmonic oscillator potential in two dimensions [Problem 13 of Chap. 6 and (7.45)]. Indeed, many properties of quantum dots can be accounted for by means of a parabolic confinement in the xy plane and assuming an oblate shape for the dot.

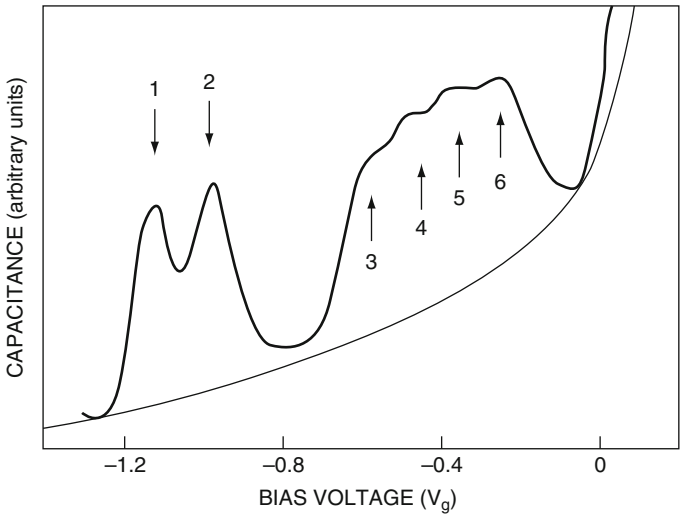

Fig. 7.5 Capacitance spectroscopy reveals quantum-dot electron occupancy and ground-state energies. (Reproduced with permission from [45])

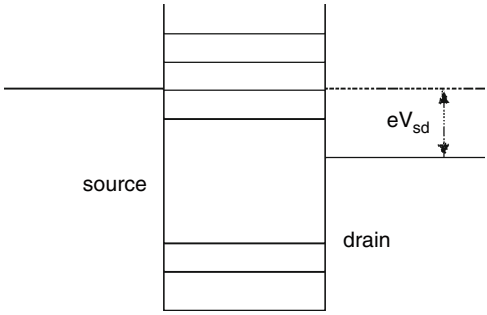

Fig. 7.6 Discrete energy levels of a quantum dot are detected by varying V_{sd}. Every time a new discrete state is accessible there is a peak in dI/dV_{sd} [44]

Being finite-size systems, quantum dots can display shell effects similar to those discussed in Sect. 7.3. One can obtain the energy spectrum by measuring the tunneling current. The Fermi level in the source rises proportionally to a voltage V_{sd} relatively to the drain and to the energy levels of the dot. Additional current flows each time that the Fermi energy of the source rises above a level of the dot. Thus energy levels are measured by the voltages at which there are peaks in the curve representing dI/dV_{sd} against V_{sd}, where I is the tunneling current (Fig. 7.6).

Energy levels vary also in the presence of a magnetic field perpendicular to the GaAs layer. Very strong fields may produce Landau levels (Sect. 7.6.1†).

Quantum dots also display spin filtering capabilities for generating or detecting spin-polarized currents [45]. In one of such devices the spin state is mapped into a charge state as follows: the splitting between the energy levels is made so large that only the ground state can be occupied. Moreover, Coulomb repulsion ensures that

at most one electron is allowed. A magnetic field lifts the degeneracy between the spin-up and spin-down states by an amount larger than the thermal energy. Initially the Fermi level ϵ_F of an adjacent reservoir lies below the spin-up state and the dot is empty. The voltage is then adjusted so ϵ_F lies in between the two spin states. Thus an electron with spin up remains in the dot, while an electron with spin down leaves the dot. Subsequently, the charged state is measured. Once emptied, the dot can receive another electron with spin up from the reservoir.

This device constitutes a modern version of the Stern–Gerlach apparatus. It joins several advances in the electrical control of spins, including electrically controlled coupling between spins in quantum dots, quasi-one-dimensional quantum-dot arrays, etc. Since such devices could be self-contained in a chip (without the need of lasers and other optical elements) they could interface naturally with conventional electronic circuits. Thus they may be essential elements in future instrumentation for quantum information.

Another application is based on the emission frequency sensitivity to the size and composition of the dot. As a consequence, quantum dots have shown advantages over traditional organic dyes in modern biological analysis. They also allow for the use of blue lasers in modern DVD players.

7.5† Bose–Einstein Condensation

In 1924, Einstein realized the validity of the fact that as T increases (and remains below a critical value T_c), the ground state of a system of bosons (particles at rest) remains multiply occupied (see Sect. 7.7†) [46]. Any other single orbital, including the orbital of the second lowest energy, will be occupied by a relatively negligible number of particles. This effect is called Bose–Einstein condensation.[9] Its experimental realization was made possible by the development of techniques for cooling, trapping and manipulating atoms.[10]

In Einstein's original prediction, all bosons were supposed to be slowed down to zero momentum, which implies a macroscopic space, according to the uncertainty principle. However, any experimental set-up requires some confinement. The confining potential in the available magnetic traps for alkali atoms can be safely approximated by the quadratic form

$$V_{\text{ext}}(\boldsymbol{r}) = \frac{M\omega^2}{2} r^2. \tag{7.40}$$

[9]The sources [47] have been used for this section.

[10]Einstein himself suggested H_2 and He^4 as possible candidates for B–E condensation. Only in 1938 the He^4 superfluid transition at 2.4 K was interpreted as a transition to the B–E condensate. However, this interpretation was marred by the presence of large residual interactions.

Neglecting the interaction between atoms implies that the Hamiltonian eigenvalues have the form (6.31), since we are considering a system composed of a large number ν of non-interacting bosons. The many-body ground state $\varphi(\boldsymbol{r}_1, \ldots, \boldsymbol{r}_\nu)$ is obtained by putting all the particles into the lowest single-particle state $\varphi_0(\boldsymbol{r})$:

$$\varphi(\boldsymbol{r}_1, \ldots, \boldsymbol{r}_\nu) = \prod_{i=1}^{i=\nu} \varphi_0(\boldsymbol{r}_i), \qquad \varphi_0(\boldsymbol{r}) = \left(\frac{M\omega}{\pi\hbar}\right)^{3/4} \exp(-r^2/2x_c^2). \tag{7.41}$$

The density distribution then becomes $\rho(\boldsymbol{r}) = \nu\,|\varphi_0(\boldsymbol{r})|^2$. While its value grows with ν, the size of the cloud is independent of ν and is fixed by the harmonic oscillator length x_c (3.28). It is typically of the order of $x_c \approx 1\ \mu$m in today's experiments.

At finite temperatures, particles are thermally distributed among the available states. A rough estimate may be obtained by assuming $k_B T \gg \hbar\omega$. In this limit we may use a classical Boltzmann distribution

$$n(\boldsymbol{r}) = \exp\left(-M\omega^2 \boldsymbol{r}^2/2k_B T\right), \tag{7.42}$$

which displays the much broader width

$$\frac{k_B T}{M\omega^2} = x_c \frac{k_B T}{\hbar\omega} \gg x_c. \tag{7.43}$$

Therefore, the Bose–Einstein condensation in harmonic traps appears as a sharp peak in the central region of the density distribution. Figure 7.7 displays the density for 5,000 non-interacting bosons in a spherical trap at temperature $T = 0.9T_c$, where T_c is the critical temperature (see below). The central peak is the condensate, superimposed on the broader thermal distribution. The momentum distribution of the condensate is also Gaussian, having a width $\hbar/x_c$ (3.46). The momentum distribution of the thermal particles is broader, of the order of $(k_B T)^{1/2}$. In fact these two momentum distributions are also represented by the curves in Fig. 7.7, provided the correct units are substituted.

In 1995, rubidium atoms confined within a magnetic trap were cooled to the submicrokelvin regime by laser methods and then by evaporation [48]. The trap was suddenly turned off, allowing the atoms to fly away. By taking pictures of the cloud after various time delays, a two-dimensional momentum distribution of the atoms was constructed. As the temperature was lowered, the familiar Gaussian hump of the Maxwell–Boltzmann distribution was pierced by a rapidly rising sharp peak caused by atoms in the ground state of the trap, that is by the condensate.

By allowing the trap to have cylindrical symmetry, the average momentum along the short axis was double that along the other [see the harmonic oscillator predictions (3.46)]. In contrast, the momentum distribution is always isotropic for a classical gas, unless it is flowing.

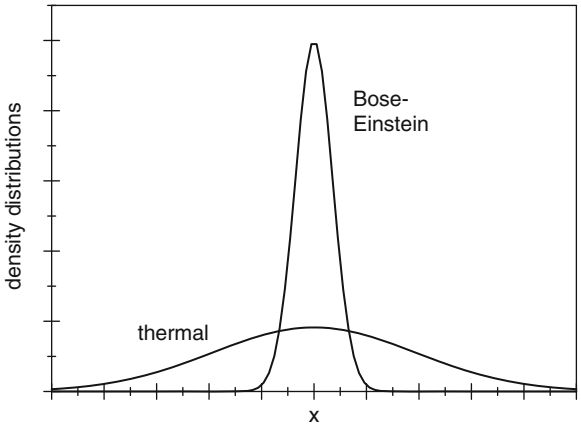

Fig. 7.7 Comparison between the densities of the condensate and the thermal particles

The calculation of the critical temperature T_c involves concepts of statistical mechanics that lie beyond the scope of this discussion. The experimental results for the condensate fraction closely follow the thermodynamic limit [48]:

$$\frac{T}{T_c} = 1 - \left(\frac{\nu_0}{\nu}\right)^{1/3}.$$

For 40,000 particles, T_c is approximately 3×10^{-7} K.

The first demonstration of the Bose–Einstein condensation involved 2,000 atoms. Today millions are being condensed.

Bose–Einstein condensation is unique because it is the only pure quantum mechanical phase transition: it takes place without any interaction between the particles. This field is presently full of activity: collective motion, condensation and damping times of the condensate, its interaction with light, collision properties, and effects of the residual interactions are just some of the themes that are currently under very intense theoretical and experimental study.

7.6† Quantum Hall Effects

A planar sample of conductive material is placed in a magnetic field perpendicular to its surface. An electric current I is made to pass from one end to the other by means of a potential V_L. The longitudinal resistivity is the ratio $R_L = V_L/I$. Because of the Lorentz force, more electrons accumulate on one side of the sample than on the other, thereby producing a measurable voltage V_H – the Hall voltage – across the sample. The ratio $R_H = V_H/I$ is called the Hall resistivity. It increases linearly with the magnetic field.

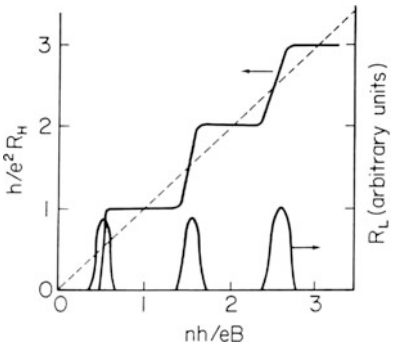

Fig. 7.8 The integer quantum Hall effect appears as plateaus in the Hall resistivity of a sample which coincide with the disappearance of the sample's electrical resistivity, as the magnetic field strength is varied [51]. (Reproduced with permission from Springer-Verlag)

However, in 1980 Klaus von Klitzing found that, for samples cooled to within 1 K and placed in strong magnetic fields, the Hall resistivity exhibits a series of plateaus, i.e. intervals in which the Hall resistivity appears not to vary at all with the magnetic field [49]. Figure 7.8 displays a diagram of the measured inverse Hall resistance $h/e^2 R_{\mathrm{H}}$ as a function of the density of electrons n times the characteristic area of the problem (7.48). The longitudinal resistance is sketched as well. Where the Hall resistivity is constant, the longitudinal resistivity practically vanishes. Moreover, the resistivity is $R_{\mathrm{H}} = h/e^2 n$, with an amazing accuracy of order 10^{-6}. Here h is Planck's constant, e is the electron charge and n is an integer (Fig. 7.8). This is even true for samples with different geometries and with different processing histories, as well as for a variety of materials. It is the integer quantum Hall effect.

In 1982 Daniel Tsui, Horst Störmer and Arthur Gossard discovered other plateaus at which n has specific fractional values (1/3, 2/5 and 3/7) [50]. This is the fractional quantum Hall effect.

7.6.1† Integer Quantum Hall Effect

Consider the planar motion of an electron in an external, uniform, magnetic field perpendicular to the plane.[11] For the sake of simplicity we will study circular geometries, and thus choose the symmetric gauge $A_x = yB/2$, $A_y = -xB/2$. Replacing the momentum $\hat{\boldsymbol{p}}$ by the effective momentum $\hat{\boldsymbol{p}} - e\boldsymbol{A}$ [53] in the free particle Hamiltonian yields

$$\hat{H} = \frac{1}{2M}\hat{\boldsymbol{p}}^2 + \frac{e^2 B^2}{8M}\rho^2 + \frac{\mu_{\mathrm{B}} B}{\hbar}\left(\hat{L}_z + 2\hat{S}_z\right). \tag{7.44}$$

[11] The main source of this section is [52].

The first two terms in (7.44) represent a two-dimensional harmonic Hamiltonian. The eigenvalues and eigenstates of the two-dimensional harmonic oscillator are (see Problem 13 in Chap. 6)

$$\begin{aligned} E_n &= \hbar\omega(n+1), \qquad n = 0, 1, 2, \ldots, \qquad x_\mathrm{c} = \sqrt{\hbar/M\omega} \\ \varphi_{nm_l}(\rho,\phi) &= R_{n_\rho m_l}(u)\varphi_{m_l}(\phi),\ \rho = \sqrt{x^2+y^2},\ \phi = \tan^{-1}\frac{y}{x},\ u = \rho/x_\mathrm{c} \\ \varphi_{m_l}(\phi) &= \frac{1}{\sqrt{2\pi}}\exp(\mathrm{i}m_l\phi), \qquad m_l = n, n-2, \ldots, -n \\ R_{n_\rho m_l}(u) &= N_{nm_l}\exp(-u^2/2)u^{m_l}f_{n_\rho m_l}(u^2), \qquad n_\rho = \frac{1}{2}(n-m_l). \end{aligned} \tag{7.45}$$

The first two terms in (7.44) yield the frequency

$$\omega = -\frac{eB}{2M} = \frac{\mu_\mathrm{B}B}{\hbar}. \tag{7.46}$$

The term proportional to $\hat{L}_z$ arises from the cross product of the square of the effective momentum, and the term proportional to $\hat{S}_z$ arises from (5.22). Since the change in energy produced by increasing n by one unit is exactly compensated by decreasing the orbital angular momentum by one unit of $\hbar$, there are sets of degenerate states called Landau levels. In particular, the lowest Landau level is made up of radial nodeless states and values of $m_l = -n$. It has zero energy, since the spin term ($s_z = -\hbar/2$) compensates exactly for the zero point energy $\hbar\omega$ of the harmonic oscillator.

To keep electrons from flying apart, one adds a radial confining potential which does not alter the symmetry of the problem. Let us assume that all states of the first Landau level are occupied[12] up to and including a minimum angular momentum $|M_l|$. The expectation value of the density,

$$\sum_{n=0}^{n=|M_l|} |\varphi_{n(-n)}|^2 = \frac{2}{x_\mathrm{c}^2}\exp\left(-u^2\right)\sum_{n=0}^{n=|M_l|}\frac{1}{n!}u^{2n}, \tag{7.47}$$

is practically constant for $u \equiv \rho/x_\mathrm{c} \ll \sqrt{|M_l|}$ and drops rapidly to zero around $\sqrt{|M_l|}$. This configuration is incompressible, since a compression would require the promotion of an electron to a higher Landau level.

Since the characteristic area of the problem is

$$\pi x_\mathrm{c}^2 = \frac{\hbar\pi}{M\omega} = \frac{h}{|e|B}, \tag{7.48}$$

[12]The Slater determinant for $|M_l|+1$ electrons moving in the first Landau level is written in (7.50).

the constant of proportionality between the number of electrons per unit area and the strength of the magnetic field depends only on Planck's constant and the charge of the electron.

However, there are impurities and, consequently, the single energy of a Landau level is spread out into a band. The states of the band belong to two classes: states near the bottom or the top of the band are localized states.[13] Near the center of each energy band are extended states, each one spreading out over a large space. They are the only ones that may carry current.

At very low temperatures, only states below the Fermi energy are occupied. Assume that the Fermi level is at the subband of localized states near the top of some Landau band. Now gradually increase the strength of the magnetic field, adjusting the current so that the Hall voltage remains constant. Since the number of states per unit area is proportional to the applied magnetic field [see (7.48)], the number of levels in each Landau state increases proportionately.

Many of the newly available states will be below the Fermi level, so electrons from higher energy localized states will drop to fill them. As a result, the Fermi level descends to a lower position. However, as long as it remains in the subband of high-energy localized states, all the extended states remain fully occupied. The amount of current flowing therefore remains constant and so does the Hall resistivity.

As the Fermi level descends through the subband of extended states, some of them are vacated. The amount of current flowing decreases, while the Hall resistivity increases.

Eventually, the extended states will be emptied and the Fermi level will enter the subband of low-energy localized states. If there is at least one full Landau band below the Fermi level, the extended states in that band will be able to carry a constant current. However, because the extended states in one band have been completely emptied, the number of subbands of extended states has been reduced by one, and the Hall resistance is larger than it was on the previous plateau. The current is proportional to the number of occupied subbands of extended states, and on each plateau an integral number of these subbands is filled.

The second striking feature of the quantized Hall effect is that current flows without resistance in the plateau region. Recall that, to dissipate power, an electron must make a transition to a state of lower energy, the excess energy being distributed within the lattice as vibrations or heat.

First we examine the regime between two plateaus. The Fermi energy varies slightly from point to point: the voltage measured at opposite sides of the sample gauges the difference between the Fermi energies at the two points. Thus, an electron can find itself in an extended state that is below the local Fermi energy in one region of space, but which extends into a region where its energy is above the local Fermi energy. The electron would thus be able to drop into a lower level, dissipating some energy into the lattice. This sample exhibits electrical resistance.

[13] Low (high) energy localized states arise around impurity atoms which have an excess (dearth) of positive charge.

If the Fermi energy is within the region of energy corresponding to localized states, there may also be empty states of lower energy. These states, however, are far apart in space, at distances much larger than the localization distance. Electrons cannot drop to lower states, and thus they cannot dissipate energy.

Within this model, localized states also act as a reservoir of electrons, so that, for finite ranges of magnetic field strengths, the extended states in each Landau band are either completely empty or completely filled. Without the reservoir, the width of the regions displaying an integer quantum Hall effect would be vanishingly small.

Therefore, a relatively simple model of independent electrons, moving under the influence of electric and magnetic fields, can account for the main properties of the integer quantum Hall effect. This model has some features in common with the band structure of metals that explains the existence of conductors and insulators (Sect. 7.4.2†).

The quantized Hall effect enables us to calibrate instruments with extreme accuracy as well as to measure fundamental physical constants more precisely than ever before.

7.6.2† Fractional Quantum Hall Effect

The fractional quantum Hall effect is seen only when a Landau level is partially filled. For instance, a plateau is seen when the lowest Landau level is approximately one-third full. In this case the Hall resistivity is equal to one-third of the square of the electron charge divided by Planck's constant.

The independent particle model previously used to explain the integer quantum Hall effect does not show any special stability when a fraction of the states is filled. To explain the fractional quantum Hall effect, we must consider the interaction between electrons (like everything associated with open shells).

It is helpful to write the total wave function of particles moving in a Landau level as a Slater determinant (7.11):

$$\Psi = \left(\frac{\sqrt{2}}{x_c}\right)^{M_l+1} \frac{1}{\sqrt{(M_l+1)!}} \left(\prod_{n=0}^{n=M_l} \frac{1}{\sqrt{n!}}\right) \Phi(1,2,\ldots,M_l+1), \tag{7.49}$$

where

$$\Phi = \exp\left(-\frac{1}{2}\sum_{i=1}^{i=M_l+1} |z_i|^2\right) \begin{vmatrix} 1 & 1 & \cdots & 1 \\ z_1 & z_2 & \cdots & z_{M_l+1} \\ z_1^2 & z_2^2 & \cdots & z_{M_l+1}^2 \\ \vdots & \vdots & \ddots & \vdots \\ z_1^{M_l} & z_2^{M_l} & \cdots & z_{M_l+1}^{M_l} \end{vmatrix}$$

$$= \exp\left(-\frac{1}{2}\sum_{i=1}^{i=M_l+1}|z_i|^2\right)\prod_{i>j=0}^{i>j=M_l-1}(z_i - z_j). \tag{7.50}$$

Here $z \equiv u\exp(-\mathrm{i}\phi)$.

In 1983, Robert Laughlin modified this wave function as follows [54]:

$$\Phi_\nu = \exp\left(-\frac{1}{2}\sum_{i=1}^{i=M_l+1}|z_i|^2\right)\prod_{i>j=0}^{i>j=M_l-1}(z_i - z_j)^\nu. \tag{7.51}$$

These wave states are exact ground states in the limit when electron–electron repulsions become infinitely short ranged. The exponent ν measures the fraction of filled states: the wave functions have the required stability when ν equals 1/3, 1/5, 1/7, 2/3, 4/5 or 6/7. The denominator in the fraction ν must be an odd number to satisfy the Pauli principle. A mechanism based on localized and extended states may also be invoked here but, instead of being applied to independent electrons, it must be used for quasi-particles, which may be described as fractionally charged anyons (see the first footnote 1 on p. 111). The topic of anyons lies beyond the scope of this text.

7.7† Quantum Statistics

Differences between counting the number of states according to whether the particles are distinguishable or not and, in the latter case, whether they are bosons or fermions, have already appeared in the two-body case, as shown in Sect. 7.1. If three particles have to be distributed into three states, we may construct:

- One antisymmetric Slater determinant (7.11)
- Ten symmetric states [three states $\varphi_a^{(3)}$, six states $\varphi_a^{(2)}\varphi_b^{(1)}$ and one state $\varphi_a^{(1)}\varphi_b^{(1)}\varphi_c^{(1)}$ (7.9)]
- Sixteen states which are neither symmetric nor antisymmetric

Such differences lead to different occupation distributions $n(\epsilon)$ for the levels with energy ϵ.[14] Let us assume that:

1. The equilibrium distribution is the most probable distribution consistent with a constant number of particles and a constant energy.
2. The particles are identical.
3. The particles are distinguishable.
4. There is no restriction on the number of particles in any state.

[14] See [58], p. 417.

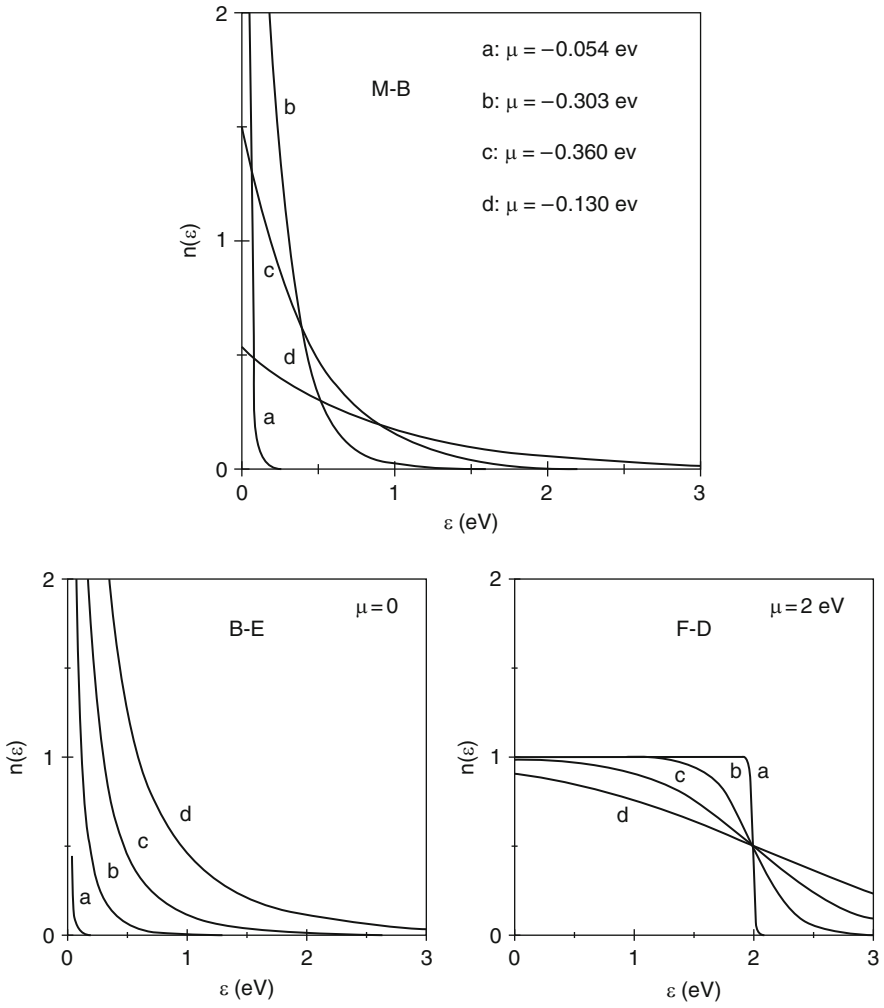

Fig. 7.9 Maxwell–Boltzmann (M–B), Bose–Einstein (B–E) and Fermi–Dirac (F–D) distribution functions. The value $n(\epsilon)$ gives the fraction of levels at a given energy which are occupied when the system is in thermal equilibrium. The curves correspond to (a) $T = 300\,\mathrm{K}$, (b) $T = 1{,}000\,\mathrm{K}$, (c) $T = 5{,}000\,\mathrm{K}$ and (d) $T = 10{,}000\,\mathrm{K}$

Given these assumptions, one derives the classical M–B distribution [Fig. 7.9 (M–B)]:

$$\eta(\epsilon) = \exp\left(-\frac{\epsilon - \mu}{k_\mathrm{B} T}\right), \tag{7.52}$$

where μ is a constant fixing the number of particles.

In the quantum mechanical case, this distribution can only hold if the particles do not overlap. If this is not the case and, consequently, assumption 3 is removed, one obtains the B–E distribution [Fig. 7.9(B–E)], which applies to bosons [55]

$$\eta(\epsilon) = \left[\exp\left(\frac{\epsilon - \mu}{k_\mathrm{B} T}\right) - 1\right]^{-1}. \tag{7.53}$$

The occupancy of the ground state equals the total number of particles in the limit $T \to 0$. If we choose zero for the energy of the ground state,

$$\lim_{T\to 0} \eta(0) = \lim_{T\to 0} \left(1 - \frac{\mu}{k_\mathrm{B} T} + \cdots - 1\right)^{-1} \approx -\frac{k_\mathrm{B} T}{\mu} \approx N, \qquad \mu = -\frac{k_\mathrm{B} T}{N}. \tag{7.54}$$

Thus, in a boson system, the constant μ must lie below the ground state energy, if the occupations are to be non-negative numbers. In Fig. 7.9(B–E) it is assumed that $k_\mathrm{B} T \ll N$.

Moreover, if assumption 4 is replaced by the condition that the number of particles in each level may be 0 or 1, the F–D distribution is derived [Fig. 7.9 (F–D)] [56, 57]

$$\eta(\epsilon) = \left[\exp\left(\frac{\epsilon - \mu}{k_\mathrm{B} T}\right) + 1\right]^{-1}. \tag{7.55}$$

In the case of an electron gas, the parameter μ may be approximated by the Fermi energy ϵ_F for $T \approx 0$ (Sect. 7.4.1). Thus $\mu \approx 3.23\,\mathrm{eV}$ for the Na case.

At energies below $k_\mathrm{B} T$, the number of particles per quantum state is greater for the B–E than for the M–B distribution. The opposite is true for the F–D distribution. For small temperatures, this last distribution only differs from a step function within a region of a few $k_\mathrm{B} T$ around $\epsilon = \mu$. This fact can be exploited by expanding the integrand $g(\epsilon)\,\eta(\epsilon)$ around μ. The first terms in the resultant Sommerfeld expansion are

$$\int_{-\infty}^{\infty} g(\epsilon)\eta(\epsilon)\mathrm{d}\epsilon = \int_{-\infty}^{\mu} g(\epsilon)\mathrm{d}\epsilon + \frac{\pi^2}{6}(k_\mathrm{B} T)^2 \left.\frac{\mathrm{d}g}{\mathrm{d}\epsilon}\right|_{\epsilon=\mu} + \mathcal{O}\left(\frac{k_\mathrm{B} T}{\mu}\right)^4. \tag{7.56}$$

For values of $(\epsilon - \mu)/k_\mathrm{B} T \gg 1$, the three distributions coincide.

7.8† Occupation Number Representation (Second Quantization)

The representation (3.37) of the harmonic oscillator states may be straightforwardly generalized to the case in which ν oscillators are present. The eigenstates and eigenvalues of the energy are [see (7.1)]

$$\varphi_{n_1,n_2,\ldots,n_\nu} = \prod_{p=1}^{p=\nu} \frac{1}{\sqrt{n_p!}} (a_p^+)^{n_p} \varphi_0, \qquad a_p \varphi_0 = 0,$$

$$E_{n_1,n_2,\ldots,n_\nu} = \sum_{p=1}^{p=\nu} E_p n_p, \tag{7.57}$$

where n_p is an eigenvalue of the operator $\hat{n}_p = a_p^+ a_p$ ($n_p = 0, 1, 2, \ldots$). We have disregarded the ground state energy.

The creation and annihilation operators corresponding to different subscripts commute with each other

$$[a_p, a_q] = \left[a_p^+, a_q^+\right] = 0, \qquad \left[a_p, a_q^+\right] = \delta_{pq}. \tag{7.58}$$

The n_p quanta that occupy the p-state are indistinguishable from one another. They are therefore bosons, and states $\varphi_{n_1,n_2,\ldots,n_\nu}$ constitute another representation of states (7.10). Note that it is much simpler to construct the vector state (7.57) than to apply the symmetrization operator $\hat{\mathcal{S}}$ (7.8). Examples of the occupation number representation are given by phonons in lattice structures (Sect. 7.4.4†) and by the quantized radiation field (Sect. 9.8.2†).

One-body operators in many-body systems have been previously expressed as a sum of individual terms $\hat{Q} = \sum_i \hat{Q}_i$. In second quantization we may write $\hat{Q} = \sum_{q \cdot p} c_{qp} a_q^+ a_p$

$$\begin{aligned} \langle n_1, n_2, \ldots, (n_q + 1), (n_p - 1), \ldots, n_\nu | Q | n_1, n_2, \ldots, n_q, n_p \ldots n_\nu \rangle \qquad (7.59) \\ = \langle (n_q + 1), (n_p - 1) | Q | n_q, n_p \rangle \\ = c_{qp} \sqrt{(n_q + 1)(n_p)} \\ = c_{qp} \quad \text{if} \quad n_p = 1, \; n_q = 0. \end{aligned}$$

Therefore, $c_{qp} = \langle q | Q | p \rangle$ and thus

$$\hat{Q} = \sum_{qp} \langle q | Q | p \rangle a_q^+ a_p. \tag{7.60}$$

This expression makes no explicit reference to individual particles. A similar equivalence may be obtained for n-body operators. If $n = 2$,

$$\hat{Q} = \frac{1}{2} \sum_{\mu\nu\eta\zeta} \langle \varphi_\mu(1) \varphi_\nu(2) | v(1,2) | \varphi_\eta(1) \varphi_\zeta(2) \rangle a_\mu^+ a_\nu^+ a_\zeta a_\eta. \tag{7.61}$$

The operators $a_{lm_l}^+$ and $(-1)^{l-m_l} a_{l(-m_l)}$ have the same coupling properties as the spherical harmonics Y_{lm_l}.

Another important advantage of the second quantization formalism becomes apparent if the number of particles is not conserved. If an atom is prepared in an exited state, after a finite time the quantum state will be a superposition of a

component representing the initial state plus another component with the atom in a lower state and an emitted photon. The number of photons is not conserved.

It is natural to seek a similar formalism which may apply to fermions. A system of such particles can be described as a many-particle state vector that changes its sign with the interchange of any two particles. Since the required linear combination of products of one-particle states [Slater determinant (7.11)] can be uniquely specified by listing the singly occupied states, the formalism we seek must limit the eigenvalues of $\hat{n}_p$ to 0 and 1.

The desired modification consists in the replacement of commutators $[\hat{A}, \hat{B}]$ by anticommutators

$$\{\hat{A}, \hat{B}\} \equiv \hat{A}\hat{B} + \hat{B}\hat{A}. \tag{7.62}$$

The anticommutators of creation and annihilation operators read

$$\{a_p, a_q\} = \{a_p^+, a_q^+\} = 0, \qquad \{a_p^+, a_q\} = \delta_{pq}. \tag{7.63}$$

The eigenvalues of the number operators are obtained by constructing the operator equation

$$(\hat{n}_p)^2 = a_p^+ a_p a_p^+ a_p = a_p^+ (1 - a_p^+ a_p) a_p = a_p^+ a_p = \hat{n}_p. \tag{7.64}$$

Since both operators $(\hat{n}_p)^2$ and $\hat{n}_p$ are simultaneously diagonal, (7.64) is equivalent to the algebraic equation $n_p^2 = n_p$, which has two roots: 0 and 1. Fermions thus obey the exclusion principle. Within this limitation, the eigenstates and energies (7.57) are also valid for the case of fermions. Note that an interchange of two fermion creation operators changes the sign of the eigenststate [as happens for the Slater determinant (7.11)].

A state such as a closed shell, in which levels μ are occupied, may be represented as

$$\varphi_0 = \prod_\mu a_\mu^+ \, \varphi_{\text{vacuum}}. \tag{7.65}$$

φ_0 may be used as a redefined vacuum state. Thus $a_\eta^+ \varphi_0$ and $a_\eta^+ a_\mu \varphi_0$ represent a one-particle state and a particle-hole state, respectively.

Single-body and two-body operators are also constructed as in (7.60) and (7.61) within the fermion occupation number representation. If acting on products of fermion creation and annihilation operators, care must be taken with the number of permutations between the operators, to obtain consistent phases.

The operators a_{jm}^+ and $(-1)^{j-m} a_{j(-m)}$ have the same angular momentum coupling properties as states φ_{jm}.

Problems

Problem 1. Two particles with equal mass M are confined by a one-dimensional harmonic oscillator potential characterized by the length x_c. Assume that one is in the eigenstate $n = 0$ and the other in $n = 1$. Find the probability density for the relative distance $x = x_a - x_b$, the root mean square value of x, and the probability of finding the two particles within a distance of $x_c/5$ from each other if they are:

1. Non-identical particles
2. Identical bosons
3. Identical fermions

Hint: write the two-particle wave function in terms of the relative coordinate x and the center of mass coordinate $x_g = (x_a + x_b)/2$ and integrate the total probability density with respect to x_g.

Problem 2. Consider a He atom in which one electron is in the state $\varphi_{100\frac{1}{2}m_s}$ and the other in the state $\varphi_{21m_l\frac{1}{2}m_s}$.

1. Construct the possible two-electron states.
2. Split the energy of the allowed states in a qualitative manner by including a Coulomb repulsion between the electrons.

Problem 3. Couple two independent bosons, each carrying spin 2. What spin angular momenta are possible? [See the relations (5.34)].

Problem 4. State whether the spatial sector of a two-body vector state is symmetric or antisymmetric with respect to the interchange of the particles, if the spin sector is given by [see (5.30)]:

1. $[\varphi_{\frac{1}{2}}(1)\,\varphi_{\frac{1}{2}}(2)]^0_0$
2. $[\varphi_{\frac{1}{2}}(1)\,\varphi_{\frac{1}{2}}(2)]^1_m$
3. $[\varphi_1(1)\,\varphi_1(2)]^0_0$
4. $[\varphi_1(1)\,\varphi_1(2)]^1_m$
5. $[\varphi_1(1)\,\varphi_1(2)]^2_m$

Problem 5. What angular momenta are possible for two fermions constrained to move in a j-shell? A j-shell is constituted by the set of states which has the same quantum numbers, including j, with the exception of the projection m.

Problem 6. Couple the spin states of a deuteron ($s_d = 1$) and a proton ($s_p = 1/2$). What total spins are possible:

1. If we ignore the Pauli principle?
2. If the three nucleons move within the $N = 0$ harmonic oscillator shell and the Pauli principle is taken into account? (This is approximately the He^3 ground state.)

Problem 7. Show that a closed fermion j-shell carries zero angular momentum:

1. Using the Slater determinant (7.11)
2. Using the occupation number representation (7.57) plus the anticommutation relations (7.63)

Problem 8. Calculate the angular momentum j and the parity of odd nuclei with 1, 3, 7, 9, 21 and 39 protons. Assume that the Hamiltonian used in Problem 3 of Chap. 6 is valid.

Problem 9. 1. Calculate the magnetic moment of nuclei with 3, 7 and 9 protons, for states with $m = j$. Disregard the neutron contribution.
2. Do the same for neutrons.

Problem 10. Obtain the ratio v/c for:

1. An electron in the outer shell of the Pb atom (Z = 82)
2. A neutron in the outer shell of the Pb^{208} nucleus
3. An electron with the Fermi momentum in metal Na [see (7.22)]

Problem 11. Repeat the calculation of Sect. 7.4.1 for a two-dimensional gas model.

Problem 12. Obtain the ratio between the average energy per electron and the Fermi energy for one-, two- and three-dimensional gas models.

Problem 13. The semiconductor Cu_2O displays an energy gap of 2.1 eV. If a thin sheet of this material is illuminated with white light:

1. What is the shortest wavelength that gets through?
2. What color is it?

Problem 14. Consider the Fermi–Dirac distribution (7.55):

1. Find the temperature dependence of the difference $\mu - \epsilon_F$
   Hint: impose the conservation of the number of electrons n_F
2. Evaluate this difference for Na at room temperature.

Problem 15. Obtain the temperature dependence of the specific heat due to the phonons for high values of T.

Problem 16. Find the matrix elements $\langle ab|Q|ab\rangle$, $\langle bc|Q|ab\rangle$ and $\langle ac|Q|ab\rangle$ of the operator $\hat{Q} = \sum_{pq} q_{pq} a_p^+ a_q$, where a_p^+, a_p are fermion creation and annihilation operators and $p = a, b, c$. Assume that $q_{pq} = q_{qp}$.